

ORIGINAL RESEARCH

Tracking Multiorgan Treatment Response in Systemic AL-Amyloidosis With Cardiac Magnetic Resonance Derived Extracellular Volume Mapping

Adam Ioannou, MBBS, BSc,^{a,*} Rishi K. Patel, MBBS, BSc,^{a,*} Ana Martinez-Naharro, PhD,^a Yousef Razvi, MBChB,^a Aldostefano Porcari, MD,^{a,b} David F. Hutt, BAAppS,^a Francesco Bandera, MD, PhD,^c Tushar Kotecha, PhD,^a Lucia Venneri, MD, PhD,^a Liza Chacko, MBBS, BSc,^a Paolo Massa, MD,^a Melissa Hanger, MBBS, BSc,^a Daniel Knight, PhD,^a Charlotte Manisty, MD, PhD,^d James Moon, MD, PhD,^d Cristina Quarta, MD, PhD,^a Helen Lachmann, MD,^a Carol Whelan, MD,^a Peter Kellman, PhD,^e Philip N. Hawkins, MD, PhD,^a Julian D. Gillmore, MD, PhD,^a Ashutosh Wechelakar, MD,^{a,†} Marianna Fontana, MD, PhD^{a,†}

ABSTRACT

BACKGROUND Systemic light chain amyloidosis is a multisystem disorder that commonly involves the heart, liver, and spleen. Cardiac magnetic resonance with extracellular volume (ECV) mapping provides a surrogate measure of the myocardial, liver, and spleen amyloid burden.

OBJECTIVES The purpose of this study was to assess multiorgan response to treatment using ECV mapping, and assess the association between multiorgan treatment response and prognosis.

METHODS The authors identified 351 patients who underwent baseline serum amyloid-P-component (SAP) scintigraphy and cardiac magnetic resonance at diagnosis, of which 171 had follow-up imaging.

RESULTS At diagnosis, ECV mapping demonstrated that 304 (87%) had cardiac involvement, 114 (33%) significant hepatic involvement, and 147 (42%) significant splenic involvement. Baseline myocardial and liver ECV independently predict mortality (myocardial HR: 1.03 [95% CI: 1.01-1.06]; $P = 0.009$; liver HR: 1.03; [95% CI: 1.01-1.05]; $P = 0.001$). Liver and spleen ECV correlated with amyloid load assessed by SAP scintigraphy ($R = 0.751$; $P < 0.001$; $R = 0.765$; $P < 0.001$, respectively). Serial measurements demonstrated ECV correctly identified changes in liver and spleen amyloid load derived from SAP scintigraphy in 85% and 82% of cases, respectively. At 6 months, more patients with a good hematologic response had liver (30%) and spleen (36%) ECV regression than myocardial regression (5%). By 12 months, more patients with a good response demonstrated myocardial regression (heart 32%, liver 30%, spleen 36%). Myocardial regression was associated with reduced median N-terminal probrain natriuretic peptide ($P < 0.001$), and liver regression with reduced median alkaline phosphatase ($P = 0.001$). Changes in myocardial and liver ECV, 6 months after initiating chemotherapy, independently predict mortality (myocardial HR: 1.11 [95% CI: 1.02-1.20]; $P = 0.011$; liver HR: 1.07 [95% CI: 1.01-1.13]; $P = 0.014$).

CONCLUSIONS Multiorgan ECV quantification accurately tracks treatment response and demonstrates different rates of organ regression, with the liver and spleen regressing more rapidly than the heart. Baseline myocardial and liver ECV and changes at 6 months independently predict mortality, even after adjusting for traditional predictors of prognosis. (J Am Coll Cardiol Img 2023;■:■-■) © 2023 The Authors. Published by Elsevier on behalf of the American College of Cardiology Foundation. This is an open access article under the CC BY-NC-ND license (<http://creativecommons.org/licenses/by-nc-nd/4.0/>).

**ABBREVIATIONS
AND ACRONYMS****AL** = light chain**CMR** = cardiac magnetic resonance**ECV** = extracellular volume**FLC** = free light chain**SAP** = serum amyloid P component

Systemic light chain (AL) amyloidosis occurs as a result of deposition of misfolded immunoglobulin light chains, produced by an abnormal clonal proliferation of plasma cells, in the extracellular matrix of multiple organs. AL amyloidosis frequently involves the heart, liver, and spleen. The mainstay of treatment is cytotoxic chemotherapy aimed at suppressing immunoglobulin light-chain production, halting amyloid organ deposition and allowing gradual organ recovery.¹

Characterization of organ involvement is of great clinical significance because the degree of organ involvement has important implications on treatment and prognosis. The discovery of serum amyloid P component (SAP) scintigraphy represented a major advancement in diagnosis and management of AL amyloidosis. SAP scintigraphy involves administration of ¹²⁵I-labeled purified human SAP, which has a high binding affinity to amyloid proteins, and following gamma camera acquisition, allows accurate quantification of visceral organ amyloid deposits.² SAP scintigraphy has since been histologically validated, and several studies have demonstrated the ability to accurately yield objective evidence of organ regression in response to treatment. Limitations include the use of ionizing radiation and sparse availability, with only 2 centers worldwide having the facilities to perform SAP scintigraphy.^{3,4}

Cardiac magnetic resonance (CMR) imaging and recognition of pathognomonic patterns of late gadolinium enhancement (LGE) has formed the cornerstone of nonbiopsy diagnoses of cardiac amyloidosis, whereas extracellular volume (ECV) mapping enables the myocyte and extracellular components to be measured separately, and has been shown to improve diagnostic accuracy and patient stratification.^{5,6} Myocardial ECV mapping has also demonstrated utility in monitoring the cardiac response to treatment in AL amyloidosis, with changes in myocardial ECV accurately predicting outcomes even after adjusting for known predictors.⁷

Until recently, SAP scintigraphy was the only noninvasive method of quantifying extracardiac amyloid organ infiltration; however, a novel approach involving liver and spleen ECV measurements during routine CMR has demonstrated a high diagnostic performance in determining liver and spleen involvement.⁸

The aims of this study were to assess multiorgan response to treatment using ECV mapping, and assess the association between multiorgan treatment response and prognosis.

METHODS

Study subjects comprised individuals with AL amyloidosis identified from a long-term prospective observational study of newly diagnosed patients (ALchemy) conducted at the NAC (National Amyloidosis Centre), United Kingdom (2015-2018). All patients who underwent baseline SAP scintigraphy and CMR with ECV mapping at diagnosis were eligible for inclusion. Before enrollment, the diagnosis of AL amyloidosis was confirmed by central review of histological material inclusive of Congo red staining, with amyloid subtype being confirmed by immunohistochemistry with specific antibodies or mass spectrometry.

At 6, 12, and 24 months after initiating chemotherapy, patients were reassessed with repeat imaging, and serum biomarkers. Hematologic response, cardiac N-terminal probrain natriuretic peptide (NT-proBNP) response, and liver alkaline phosphatase (ALP) response were all defined as per international consensus criteria. In brief, hematologic response was classed as complete response (CR) (normal free light chain [FLC] levels, normal kappa/lambda ratio, and negative serum immunofixation), very good partial response (VGPR) (reduction in dFLC [difference in concentration between aberrant and uninvolved class of FLC] to <40 mg/L), partial response (>50% reduction in dFLC), or no response (NR) (≤50% reduction in dFLC). For the purpose of our analysis, patients with a VGPR were further divided into patients with

From the ^aNational Amyloidosis Centre, University College London, Royal Free Campus, London, United Kingdom; ^bCenter for Diagnosis and Treatment of Cardiomyopathies, Cardiovascular Department, Azienda Sanitaria Universitaria Giuliano-Isontina (ASUGI), University of Trieste, Italy; ^cCardiology University Department, IRCCS Policlinico San Donato, Milan, Italy; ^dSt Bartholomew's Hospital, London, United Kingdom; and the ^eNational Heart, Lung and Blood Institute, National Institutes of Health, Bethesda, Maryland, USA. *Drs Ioannou and Patel contributed equally to this work as joint first authors. †Drs Wechelakar and Fontana contributed equally to this work as joint senior authors.

The authors attest they are in compliance with human studies committees and animal welfare regulations of the authors' institutions and Food and Drug Administration guidelines, including patient consent where appropriate. For more information, visit the [Author Center](#).

normal FLC (dFLC <10 mg/L and involved FLC ≤20 mg/L) and a persistent paraprotein, and patients with abnormal FLC.⁹ NT-proBNP improvement was defined as a reduction of >30% and >300 ng/L, and NT-proBNP worsening was defined as an increase of >30% and >300 ng/L. ALP improvement was defined as a reduction of >50%, and ALP worsening was defined as an increase of >50%.⁹ Of note, data from 139 patients had been included within a prior publication from our center, but the current study includes updated analysis.⁷

Patients were managed in accordance with the Declaration of Helsinki and provided written informed consent for analysis and publication of their data (REC reference 09/H0715/58). A separate ethical approval was obtained for recruitment of healthy volunteers who underwent CMR with ECV mapping, without corresponding SAP scintigraphy (REC reference 17/SC/0077).

SAP SCINTIGRAPHY. Anterior and posterior whole-body images were acquired following ¹²³I-SAP administration using a General Electric Infinia Hawkeye or Discovery 670 Gamma Camera (GE) with extended low-energy general-purpose collimators. Liver and spleen amyloid burden was scored by visual assessment into 4 categories (no visceral organ uptake on SAP scintigraphy, small, moderate, and large amyloid loads). Analysis was carried out by operators blinded to all other investigations and patient outcomes.²

CARDIAC MAGNETIC RESONANCE. All subjects underwent CMR on a 1.5-T clinical scanner with localizers, cine imaging with steady state free precession sequence, and LGE imaging. T1 measurement was performed with the use of the modified look-locker inversion recovery sequence. After a bolus of gadoterate meglumine and LGE imaging, T1 mapping was repeated 15 minutes postcontrast using the same slice locations with the modified look-locker inversion recovery sequence, to produce automated inline ECV mapping reconstruction. T1 mapping protocols used 5s(3s)3s and 4s(1s)3s(1s)2s sampling, precontrast and postcontrast, respectively.¹⁰

Image analysis was performed off-line using Osirix MD 9.0 (Bernex). Significant change in the myocardial ECV was considered as previously described as an absolute change in ECV of 0.05.⁷ For liver and spleen ECV measurements, a single region of interest (ROI) was drawn in the liver and spleen on left ventricular short-axis ECV maps. ECV error maps were used to confirm the ROI was drawn in areas with the lowest error, and nonparenchymal anatomic structures were carefully excluded. Data pertaining to a specific organ

were excluded if the organ was not imaged or imaged incompletely affecting reliability of the ROI measurement. Clinically significant liver and spleen ECV cutoffs were 0.40 and 0.39, respectively (as previously defined).⁸ The normal ECV ranges were calculated from the population of healthy volunteers (myocardium: ECV = 0.27 ± 0.02, normal range = 0.23-0.30; liver: ECV = 0.28 ± 0.02, normal range = 0.24-0.32; spleen: ECV = 0.29 ± 0.02, normal range = 0.25-0.33).

STATISTICAL ANALYSIS. Statistical analysis was performed using IBM SPSS Statistics Version 25 apart from survival analysis, which was performed using Stata Statistical Software: Release 17 (StataCorp LLC). All continuous variables were tested for normal distribution (Shapiro-Wilk test) and presented as mean ± SD or median (IQR) other than NT-proBNP, which was natural log-transformed for parametric testing. Following analysis of healthy volunteer CMR images, normal ranges were calculated as the mean ± 2 × SD. The independent Student's *t*-test or its nonparametric equivalent were used to compare the distribution of 2 groups. Comparisons between different time points within the same group were performed by paired Student's *t*-test or its nonparametric equivalent. Categorical data are presented as absolute numbers and frequencies (%) and compared using the chi-square test. Interobserver variability for SAP scintigraphy analysis was evaluated by calculating the weighted kappa and assessing according to the Landis and Koch classification. Interobserver variability for ECV measurements was assessed by calculating the intraclass correlation coefficient with 95% CIs and Bland-Altman analysis (as expressed as bias ± 2 SDs for limit of agreement). Bland-Altman plots were also constructed to assess the validity of cutoff values for the change in ECV that best determined disease regression and progression. Correlations between parameters were assessed using Pearson (*r*) or Spearman's rho as appropriate.

All mortality data were obtained via the UK Office of National Statistics. The mortality endpoint was defined as time to death from baseline for all deceased patients and time to censor date (March 7, 2022) from baseline among the remainder. When assessing the change in multiorgan ECV measurements at 6 months as predictors of prognosis, survival analysis started from the 6-month timepoint. Survival was evaluated with Cox proportional hazards regression analysis, providing estimated HRs with 95% CIs. The proportional hazards assumption was checked and confirmed. Multivariable models were used to investigate factors associated with overall survival

and all variables were selected a priori for clinical relevance. The likelihood ratio test was used to evaluate the contribution of adding explanatory variables to each of the multivariable models. Kaplan-Meier curves were constructed, with statistical significance being assessed with a log-rank test. Statistical significance was defined as $P < 0.05$, except for the paired Student's t -test or its nonparametric equivalent, where statistical significance was defined as $P < 0.01$, to avoid spuriously significant results.

RESULTS

A total of 904 patients were diagnosed with AL amyloidosis during the study period, of whom 351 patients (mean age: 65.46 ± 10.27 years; 59.5% men) underwent baseline SAP scintigraphy and CMR with ECV mapping at diagnosis. These patients along with 20 healthy volunteers (mean age: 45.60 ± 7.20 years; 80.0% men) were included. The healthy volunteers were significantly younger ($P < 0.001$) but there was no significant difference in the proportion of men ($P = 0.069$). Patients' baseline characteristics are summarized in [Table 1](#).

At diagnosis, ECV mapping demonstrated that 304 (86.7%) patients with AL amyloidosis had cardiac involvement (ECV >0.30), 114 (32.5%) patients had significant liver involvement (ECV ≥ 0.40), and 147 (41.9%) patients had significant spleen involvement (ECV ≥ 0.39). The most common patterns of organ involvement are displayed in [Figure 1](#). A total of 171 patients (mean age: 64.34 ± 10.56 years, 61.4% men) were followed up with repeat CMR imaging following initiation of first line bortezomib-based chemotherapy ([Supplemental Figure 1](#)).

Across the study period there were a total of 597 SAP scintigraphy scans with corresponding ECV mapping (including both baseline and follow-up images). There was good correlation between the liver and spleen ECV and amyloid load as assessed by SAP scintigraphy (Spearman's rho: $R = 0.751$ [95% CI: 0.713-0.784]; $P < 0.001$; $R = 0.765$ [95% CI: 0.727-0.789]; $P < 0.001$, respectively) ([Supplemental Figure 2](#)). Technical aspects regarding measurement reproducibility and the quantification of changes in the liver and spleen ECV are described in the [Supplemental Results](#) ([Supplemental Figures 3 and 4](#)).

FOLLOW-UP 6 MONTHS POSTCHEMOTHERAPY. A total of 141 patients had a repeat CMR 6 months after commencing chemotherapy. All 85 patients with a good hematologic response had an elevated myocardial ECV at diagnosis, 53 (62.4%) patients had an elevated liver ECV, and 46 (54.1%) patients had an

TABLE 1 Baseline Characteristics of All Patients with Systemic AL Amyloidosis (N = 351)

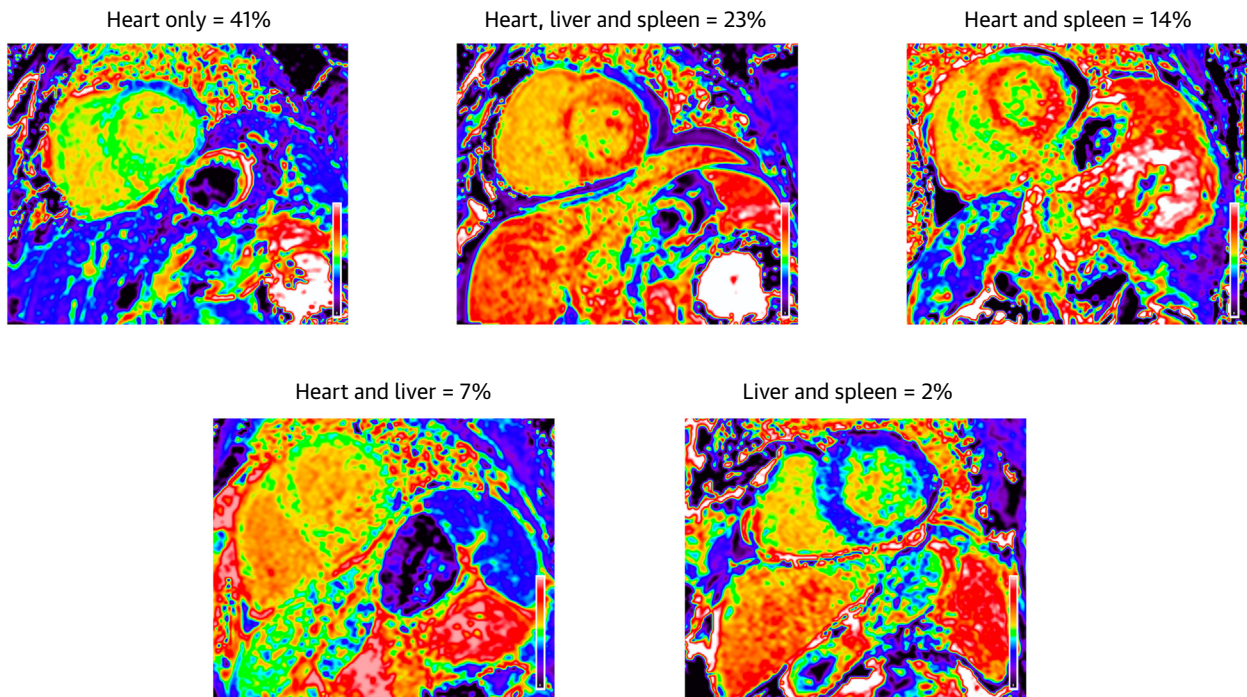
Age, y	65.46 ± 10.27
Male	209 (59.5)
Serum NT-proBNP, pg/L	2,169 (645-5,541)
Serum troponin, ng/L	48 (23-95)
Serum bilirubin, μmol/L	6 (4-10)
Serum aspartate aminotransferase, IU/L	25 (20-33)
Serum alanine aminotransferase, IU/L	26 (19-35)
Serum alkaline phosphatase, IU/L	92 (71-129)
SAP scintigraphy	
Liver uptake	93 (26.5)
Spleen uptake	195 (55.6)
Total amyloid load	
None	151 (43.0)
Small	53 (15.1)
Moderate	79 (22.5)
Large	68 (19.4)
Cardiac magnetic resonance	
LV mass, g	150.05 ± 71.82
LV mass indexed, g/m ²	80.43 ± 36.06
LV volume in diastole, mL	130.15 ± 27.52
LV volume in diastole indexed, mL/m ²	71.02 ± 29.65
LV volume in systole, mL	45.31 ± 17.19
LV volume in systole indexed, mL/m ²	24.29 ± 9.18
Stroke volume, mL	84.80 ± 17.81
Stroke volume indexed, mL/m ²	45.18 ± 8.17
Ejection fraction, %	65.62 ± 8.71
Myocardial native T ₁ , ms	1,139 (1,082-1,184)
Myocardial T ₂ , ms	50.87 ± 6.57
Myocardial extracellular volume	0.44 ± 0.10
Liver and spleen extracellular volume	
Liver extracellular volume	0.39 ± 0.12
Spleen extracellular volume	0.43 ± 0.17

Values are mean ± SD, median (IQR), or n (%).

AL = light chain; LV = left ventricular; NT-proBNP = N-terminal probrain natriuretic peptide; SAP = serum amyloid P component.

elevated spleen ECV. Myocardial ECV regression was detectable in 4 (4.7%) patients, liver ECV regression in 8 (15.1%) patients, and spleen ECV regression in 9 (19.6%) patients. Only patients with a CR achieved myocardial ECV regression, whereas some patients with a VGPR achieved liver and spleen ECV regression. Most patients with a good hematologic response had stable myocardial, liver, and spleen ECVs. However, 18 (21.2%) patients with a good hematologic response demonstrated myocardial ECV progression, compared with few demonstrating liver and spleen progression. Patients with a VGPR were divided into those with normal FLC (n = 7) but a persistent paraprotein, and those with abnormal FLC (n = 21), but this did not reveal any significant differences in multiorgan response.

Patients with a good hematologic response 6 months after initiating chemotherapy were divided

FIGURE 1 Most Common Patterns of Organ Infiltration in Systemic Immunoglobulin AL Amyloidosis

CMR-derived ECV mapping demonstrating the most common patterns of organ infiltration in systemic immunoglobulin AL amyloidosis. AL = light chain; CMR = cardiac magnetic resonance; ECV = extracellular volume.

into early response (within 3 months of starting chemotherapy) and late response (after 3 months of starting chemotherapy). All patients with myocardial ECV regression achieved an early response, whereas all patients with myocardial ECV progression achieved a late response. Most patients with liver ($n = 6$, 75.0%) and spleen ECV regression ($n = 7$, 77.8%) also achieved an early response.

In patients with a poor hematologic response, over one-half demonstrated myocardial ECV progression ($n = 27$, 65.9%), compared with only 8 (18.6%) demonstrating liver ECV progression and 6 (14.6%) demonstrating spleen ECV progression (Table 2).

A total of 103 patients underwent repeat SAP scintigraphy following 6 months of treatment. Serial ECV measurements correctly classified the change in hepatic and splenic amyloid load derived from SAP scintigraphy in 91.3% and 85.9% of cases, respectively (Figures 2 and 3).

In patients with myocardial ECV regression, there was no significant change in median NT-proBNP, but in patients with myocardial ECV progression, there

was a significant increase in median NT-proBNP (3,730 ng/L [890-6,282] vs 4,109 ng/L [1,686-11,282]; $P = 0.004$). In patients with liver ECV regression or progression there was no significant change in median ALP.

FOLLOW-UP 12 MONTHS POSTCHEMOTHERAPY.

A total of 120 patients had a repeat CMR 12 months after commencing chemotherapy. All 85 patients with a good hematologic response had an elevated myocardial ECV at diagnosis, 54 (63.5%) patients had an elevated liver ECV, and 45 (52.9%) patients had an elevated spleen ECV. Myocardial ECV regression was detectable in 27 (31.8%) patients, liver ECV regression in 16 (29.6%) patients, and spleen ECV regression in 15 (35.6%) patients. Most patients with a good hematologic response had stable myocardial, liver, and spleen ECVs. However, 10 (11.8%) patients with a good hematologic response demonstrated myocardial ECV progression, compared with few demonstrating liver and spleen progression. Patients with a VGPR were further divided into those with normal FLC

TABLE 2 Multiorgan ECV Response to Treatment 6 Months After Initiating Chemotherapy, Compared With the Hematologic Response and Repeat SAP Scintigraphy at 6 Months

All Patients Who Had Repeat CMR With ECV Mapping at 6 mo (N = 141, Liver ECV Measurable in 118 Patients and Spleen Measurable in 113 Patients)				
Hematologic Response	Complete Response (n = 57, 40.4%)	Very Good Partial Response (n = 28, 20.0%)	Partial Response (n = 36, 25.5%)	No Response (n = 20, 14.2%)
Liver ECV regression	5	3	0	0
Spleen ECV regression	7	2	0	0
Cardiac ECV regression	4	0	0	0
Stable liver ECV	44	24	24	10
Stable spleen ECV	42	20	24	11
Stable cardiac ECV	43	20	18	11
Liver ECV progression	0	0	4	4
Spleen ECV progression	0	1	3	3
Cardiac ECV progression	10	8	18	9
Patients With Repeat SAP Scintigraphy and CMR With ECV Mapping at 6 mo (N = 103, Liver ECV Measurable in 92 Patients and Spleen Measurable in 85 Patients)				
Liver Response	Liver Regression on SAP Scintigraphy (n = 3)	Stable Liver on SAP Scintigraphy (n = 84)	Liver Progression on SAP Scintigraphy (n = 5)	
Liver ECV regression	2	4	0	
Stable liver ECV	1	79	2	
Liver ECV progression	0	1	3	
Spleen Response	Spleen Regression on SAP Scintigraphy (n = 11)	Stable Spleen on SAP Scintigraphy (n = 68)	Spleen Progression on SAP Scintigraphy (n = 6)	
Spleen ECV regression	6	4	0	
Stable spleen ECV	5	63	2	
Spleen ECV progression	0	1	4	
ECV = extracellular volume; SAP = serum amyloid P component.				

(n = 4) but a persistent paraprotein and those with abnormal FLC (n = 27), but because of the small number with normal FLC, no meaningful comparisons could be made.

In patients with a poor hematologic response, nearly one-half demonstrated myocardial ECV progression (n = 16, 45.7%), compared with only 6 (20.7%) demonstrating liver ECV progression and 2 (6.5%) demonstrating spleen ECV progression.

A total of 79 patients underwent repeat SAP scintigraphy following 12 months of treatment. Serial ECV measurements correctly classified the change in hepatic and splenic amyloid load derived from SAP scintigraphy in 78.1% and 82.7% of cases, respectively (Table 3).

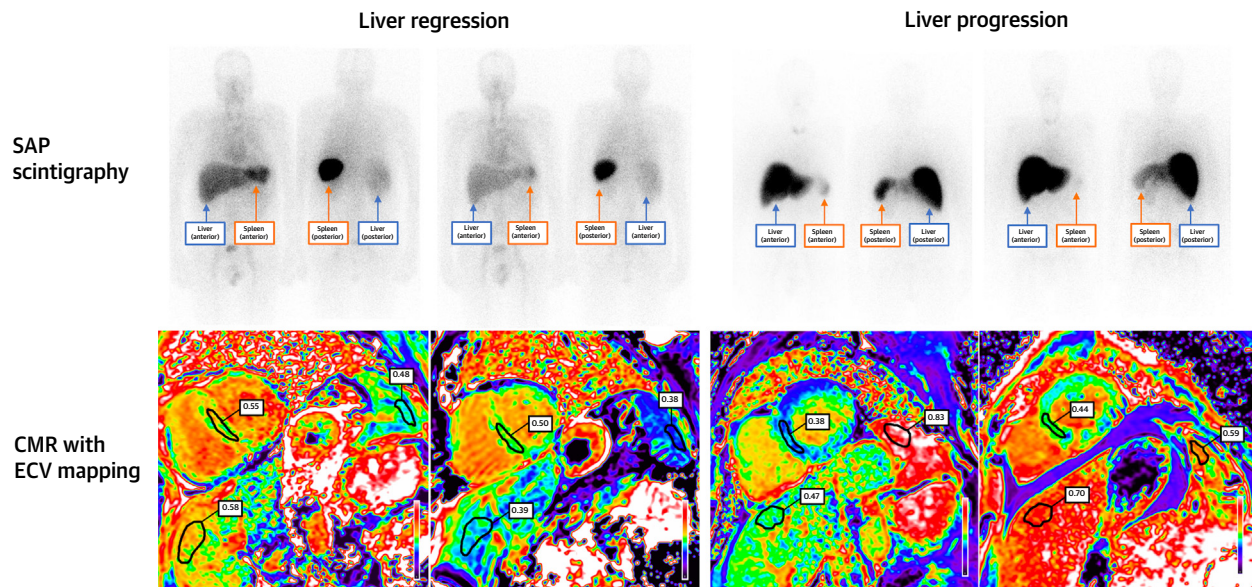
In patients with myocardial ECV regression, there was a significant reduction in median NT-proBNP, and in patients with myocardial ECV progression there was a significant increase in median NT-proBNP. In patients with liver ECV regression, there was a significant reduction in median ALP, and in patients with liver ECV progression, there was a significant increase in median ALP (Table 4).

FOLLOW-UP 24 MONTHS POSTCHEMOTHERAPY.

A total of 107 patients had a repeat CMR 24 months after commencing chemotherapy. All 86 patients with a good hematologic response had an elevated myocardial ECV at diagnosis, 54 (62.8%) patients had an elevated liver ECV, and 40 (46.5%) patients had an elevated spleen ECV. Myocardial ECV regression was detectable in 41 (47.6%) patients, liver ECV regression in 17 (31.5%) patients, and spleen ECV regression in 14 (35.0%) patients. Most remaining patients with a good hematologic response had stable myocardial, liver, and spleen ECVs. Patients with a VGPR were further divided into those with normal FLC (n = 3) but a persistent paraprotein and those with abnormal FLC (n = 28), but due to the small number with normal FLC, no meaningful comparisons could be made.

In patients with a poor hematologic response, nearly one-half demonstrated myocardial ECV progression (n = 9, 42.9%), compared with only 4 (13.8%) demonstrating liver ECV progression and 1 (6.3%) demonstrating spleen ECV progression.

A total of 64 patients underwent repeat SAP scintigraphy following 24 months of treatment. Serial

FIGURE 2 Liver Regression and Progression on SAP Scintigraphy and CMR

(Top left) Serum amyloid P component (SAP) scintigraphy demonstrating liver and spleen regression. (Bottom left) Corresponding CMR with ECV mapping demonstrating liver, spleen, and cardiac regression. (Top right) SAP scintigraphy demonstrating liver progression and spleen regression. (Bottom right) Corresponding CMR with ECV mapping demonstrating liver and cardiac progression, and spleen regression. Abbreviations as in Figure 1.

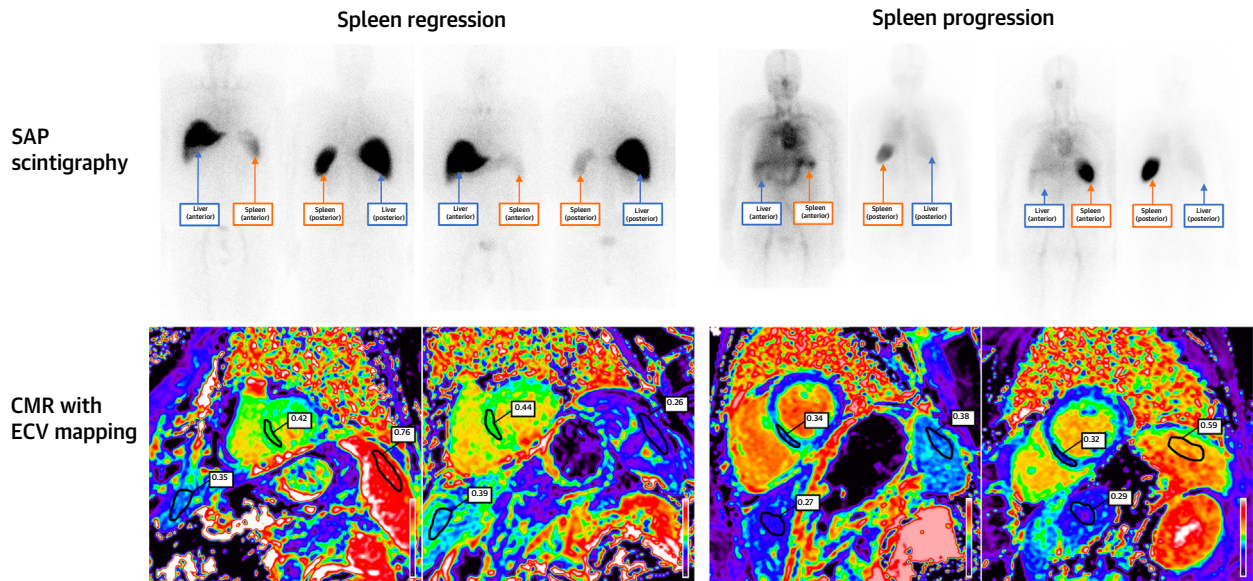
ECV measurements correctly classified the change in hepatic and splenic amyloid load derived from SAP scintigraphy in 82.0% and 74.1% of cases, respectively (Table 5).

In patients with myocardial ECV regression, there was a significant reduction in median NT-proBNP, but in patients with myocardial ECV progression, there was no significant difference in median NT-proBNP. In patients with liver ECV regression, there was a significant reduction in median ALP, but in patients with liver ECV progression, there was no significant difference in median ALP (Table 4).

SURVIVAL. At median follow-up of 52 months (IQR: 18-63 months), 134 patients from the overall population had died. Baseline myocardial ECV (measured in all 351 patients) revealed that survival probability at 24 months was 85% (95% CI: 71%-92%) in patients with a normal ECV ($ECV \leq 0.30$), 80% (95% CI: 71%-87%) in patients with a mildly elevated ECV ($ECV = 0.31-0.40$), 71% (95% CI: 62%-78%) in patients with a moderately elevated ECV ($ECV = 0.41-0.50$), and 51% (95% CI: 40%-61%) in patients with a severely elevated ECV ($ECV > 0.50$) (Figure 4A). Baseline liver ECV measurements (measurable in 342 patients) revealed that survival probability at 24 months was 83% (95% CI: 75%-89%) in patients with a normal

liver ECV ($ECV \leq 0.32$), 74% (95% CI: 64%-81%) in patients with a subclinical elevation in ECV ($ECV = 0.33-0.39$), and 56% (95% CI: 47%-65%) in patients with a clinically significant elevation in ECV ($ECV \geq 0.40$) (Figure 4B). Baseline spleen ECV (measurable in 335 patients) revealed that survival probability at 24 months was 81% (95% CI: 72%-87%) in patients with a normal spleen ECV ($ECV \leq 0.33$), 64% (95% CI: 51%-74%) in patients with a subclinical elevation in ECV ($ECV = 0.34-0.38$), and 66% (95% CI: 58%-74%) in patients with a clinically significant elevation in ECV ($ECV \geq 0.39$) (Figure 4C). Baseline myocardial ECV and liver ECV were associated with mortality, and remained independent predictors of mortality when adjusting for traditional risk factors adapted with permission from the Mayo 2012 risk stratification score (Table 6).¹¹ The likelihood ratio test demonstrated the addition of baseline liver and spleen ECV added a significant contribution to the multivariable model (chi-square = 12.24; $P = 0.002$).

At median follow-up of 51 months (IQR: 40-59 months), 40 patients from the cohort with follow-up CMR scans at 6 months had died. In patients with a stable myocardial ECV at 6 months, survival probability at 24 months was 88% (95% CI: 79%-93%), compared with 62% (95% CI: 46%-75%) in patients

FIGURE 3 Spleen Regression and Progression on SAP Scintigraphy and CMR

(Top left) SAP scintigraphy demonstrating spleen regression and a stable liver amyloid load. (Bottom left) Corresponding CMR with ECV mapping demonstrating spleen regression, and a stable liver and myocardial ECV. (Top right) SAP scintigraphy demonstrating spleen progression and no amyloid load in the liver. (Bottom right) Corresponding CMR with ECV mapping demonstrating spleen progression, a normal and stable liver ECV, and a stable myocardial ECV. Abbreviations as in Figure 1.

TABLE 3 Multiorgan ECV Response to Treatment 12 Months After Initiating Chemotherapy, Compared With the Hematologic Response and Repeat SAP Scintigraphy at 12 Months

All Patients Who Had Repeat CMR With ECV Mapping at 12 mo (N = 120, Liver ECV Measurable in 108 Patients and Spleen Measurable in 108 Patients)				
Hematologic Response	Complete Response (n = 50, 41.7%)	Very Good Partial Response (n = 35, 29.2%)	Partial Response (n = 24, 20.0%)	No Response (n = 11, 9.2%)
Liver ECV regression	11	5	0	0
Spleen ECV regression	8	7	2	0
Cardiac ECV regression	19	8	0	0
Stable liver ECV	33	27	14	9
Stable spleen ECV	36	23	16	11
Stable cardiac ECV	25	23	12	7
Liver ECV progression	1	2	4	2
Spleen ECV progression	1	2	2	0
Cardiac ECV progression	6	4	12	4
Patients With Repeat SAP Scintigraphy and CMR with ECV Mapping at 12 mo (N = 79, Liver ECV Measurable in 73 and Spleen Measurable in 75)				
Liver Response	Liver Regression on SAP (n = 4)	Stable Liver on SAP (n = 65)	Liver Progression on SAP (n = 4)	
Liver ECV regression	2	10	0	
Stable liver ECV	2	54	1	
Liver ECV progression	0	1	3	
Spleen Response	Spleen Regression on SAP Scintigraphy (n = 11)	Stable Spleen on SAP Scintigraphy (n = 61)	Spleen Progression on SAP Scintigraphy (n = 3)	
Spleen ECV regression	7	7	0	
Stable spleen ECV	4	53	1	
Spleen ECV progression	0	1	2	

Abbreviations as in Table 2.

TABLE 4 NT-proBNP Response According to Myocardial ECV Changes at 12 and 24 Months After Initiating Chemotherapy, and ALP Response According to Liver ECV Changes at 12 and 24 Months After Initiating Chemotherapy

Change in Serum Biomarkers and ECV Measurements at 12 mo										
	Myocardial ECV Regression (n = 27)			Stable Myocardial ECV (n = 67)			Myocardial ECV Progression (n = 26)			
	Baseline	12 mo	P Value	Baseline	12 mo	P Value	Baseline	12 mo	P Value	
NT-proBNP (ng/L)	2,144 (442-6,398)	717 (153-1,861)	<0.001	2,270 (812-4,322)	1,389 (451-3,853)	0.002	1,620 (813-5,606)	3,446 (1,588-7,988)	0.003	
NT-proBNP response (change >30% and >300 ng/L)	Improved = 15 (55.5) Stable = 8 (29.7) Worse = 1 (3.7) Missing = 3 (11.1)			Improved = 24 (35.8) Stable = 25 (37.3) Worse = 14 (20.9) Missing = 4 (6.0)			Improved = 3 (11.5) Stable = 6 (23.1) Worse = 15 (58.7) Missing = 2 (7.7)			
Change in Serum Biomarkers and ECV Measurements at 24 mo										
	Myocardial ECV Regression (n = 41)			Stable Myocardial ECV (n = 52)			Myocardial ECV Progression (n = 14)			
	Baseline	24 mo	P Value	Baseline	24 mo	P Value	Baseline	24 mo	P Value	
NT-proBNP (ng/L)	2,370 (939-4,318)	653 (315-1,246)	<0.001	2,327 (471-2,840)	1,411 (420-3,727)	0.018	955 (735-5,557)	2,396 (1,431-3,928)	0.191	
NT-proBNP response (change >30% and >300 ng/L)	Improved = 29 (70.7) Stable = 7 (17.1) Worse = 2 (4.9) Missing = 3 (7.3)			Improved = 16 (30.8) Stable = 23 (44.2) Worse = 9 (17.3) Missing = 4 (7.7)			Improved = 2 (14.3) Stable = 5 (35.7) Worse = 7 (50.0) Missing = 0 (0.0)			
	Liver ECV Regression (n = 17)			Stable Liver ECV (n = 70)			Liver ECV Progression (n = 8)			
	Baseline	24 mo	P Value	Baseline	24 mo	P Value	Baseline	24 mo	P Value	
ALP (IU/L)	177 (98-252)	102 (73-149)	0.001	88 (71-120)	96 (76-122)	0.235	80 (79-98)	113 (111-162)	0.008	
ALP response (change >50%)	Improved = 4 (25.0) Stable = 12 (75.0) Worse = 0 (0.0) Missing = 0 (0.0)			Improved = 2 (2.4) Stable = 65 (78.3) Worse = 13 (15.7) Missing = 3 (3.6)			Improved = 0 (0.0) Stable = 6 (66.6) Worse = 3 (33.3) Missing = 0 (0.0)			
Values are n (%) or median (IQR). ALP = alkaline phosphatase; NT-proBNP = N-terminal probrain natriuretic peptide; other abbreviations as in Table 2.										

with myocardial ECV progression (Figure 5A). In patients with a stable liver ECV at 6 months, survival probability at 24 months was 84% (95% CI: 76%-90%), compared with 25% (95% CI: 4%-56%) in patients with liver ECV progression (Figure 5B). In patients with a stable spleen ECV at 6 months, survival probability at 24 months was 86% (95% CI: 77%-91%) compared with 29% (95% CI: 4%-61%) in patients with spleen ECV progression (Figure 5C). Multivariable analysis adjusting for hematologic response; NT-proBNP response; and change in myocardial, liver, and spleen ECV demonstrated that change in myocardial ECV and liver ECV remained independent predictors of prognosis (Table 6). The likelihood ratio test demonstrated the addition of change in liver and spleen ECV added a significant contribution to the multivariable model (chi-square = 9.94; $P = 0.007$). In the subgroup of 37 patients with normal SAP scintigraphy (no visceral organ uptake) at baseline and at 6 months there were 5 deaths, and neither change in

liver ECV (HR: 1.08 [95% CI: 0.74-1.56]; $P = 0.705$) or spleen ECV (HR: 2.61 [95% CI: 0.67-10.19]; $P = 0.166$) were predictors of mortality, but change in myocardial ECV remained a predictor of mortality (HR: 1.42 [95% CI: 1.09-1.85]; $P = 0.010$).

DISCUSSION

This is the first study to assess the ability of CMR-derived ECV mapping in tracking multiorgan response to chemotherapy in AL amyloidosis. Our study demonstrated the following: 1) multiorgan ECV measurements at diagnosis predict prognosis, with myocardial and liver ECV independently correlating with mortality; 2) serial multiorgan ECV measurements track changes in response to chemotherapy, with ECV changes most likely representing changes in multiorgan amyloid burden; 3) different organs demonstrate different rates of ECV regression and progression, with the heart showing slower

TABLE 5 Multiorgan ECV Response to Treatment 24 Months After Initiating Chemotherapy, Compared With the Hematologic Response and Repeat SAP Scintigraphy at 24 Months

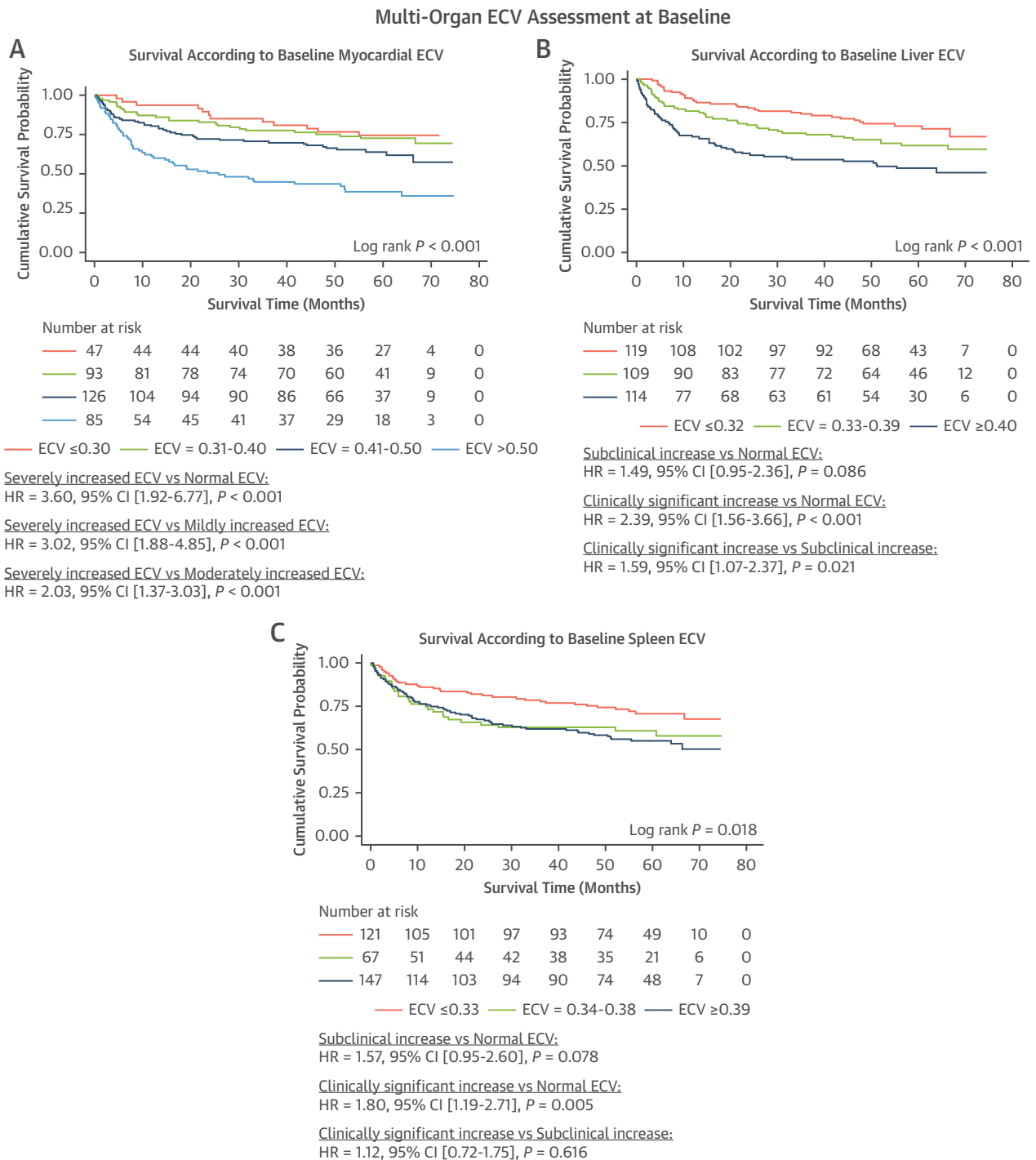
All Patients Who Had Repeat CMR With ECV Mapping at 24 mo (N = 107, Liver ECV Measurable in 95 Patients and Spleen Measurable in 94 Patients)				
Hematologic Response	Complete Response (n = 55, 51.4%)	Very Good Partial Response (n = 31, 29.0%)	Partial Response (n = 17, 15.0%)	No Response (n = 4, 3.7%)
Liver ECV regression	14	3	0	0
Spleen ECV regression	8	6	1	0
Cardiac ECV regression	30	11	0	0
Stable liver ECV	33	23	11	3
Stable spleen ECV	41	22	12	2
Stable cardiac ECV	24	18	8	2
Liver ECV progression	1	3	4	0
Spleen ECV progression	0	1	1	0
Cardiac ECV progression	1	2	9	2
Patients With Repeat SAP Scintigraphy and CMR With ECV Mapping at 24 mo (N = 64, Liver ECV Measurable in 61 and Spleen Measurable in 58)				
Liver Response	Liver Regression on SAP (n = 2)	Stable Liver on SAP (n = 56)	Liver Progression on SAP (n = 3)	
Liver ECV regression	2	8	0	
Stable liver ECV	0	46	1	
Liver ECV progression	0	2	2	
Spleen Response	Spleen Regression on SAP Scintigraphy (n = 15)	Stable Spleen on SAP Scintigraphy (n = 42)	Spleen Progression on SAP Scintigraphy (n = 1)	
Spleen ECV regression	8	6	0	
Stable spleen ECV	7	34	0	
Spleen ECV progression	0	2	1	
Abbreviations as in Table 2.				

regression and faster progression than the liver and spleen; and 4) changes in multiorgan ECV predict prognosis, with changes in myocardial and liver ECV independently correlating with mortality.

The pattern of organ involvement in AL amyloidosis has a significant impact on prognosis. However, determining organ involvement can be challenging. Serum biomarkers that reflect organ function are commonly used as surrogates to estimate the presence of amyloid infiltration. Serum cardiac enzymes are commonly used to assess myocardial infiltration, and serum ALP to assess liver infiltration, whereas there is no equivalent serum biomarker to assess spleen infiltration.¹² SAP scintigraphy has a high sensitivity and specificity for identifying liver and spleen amyloid infiltration, but cannot assess the presence of myocardial infiltration, and has sparse availability.² CMR with gadolinium contrast administration allows the isolation of signal from the extracellular space, and subsequent construction of ECV maps enables quantification of multiorgan ECVs.^{8,10} Amyloidosis is the exemplary interstitial disease, whereby amyloid deposits within the extracellular matrix causing expansion of the ECV.¹ Therefore, a global increase in ECV is most likely to represent an increase in amyloid burden.⁶ This widely

accessible imaging modality, which uses routine cardiac protocols, can easily be adopted into the clinical setting without the need for additional image acquisition or postprocessing. Multiorgan ECV mapping can identify patterns of organ involvement and accurately stratify a patient's prognosis, with both myocardial ECV and liver ECV remaining powerful independent predictors of mortality, even after adjusting for traditional prognosticators (Central Illustration).

Serial multiorgan ECV measurements are able to track changes in response to chemotherapy, and this has been validated against traditional markers of treatment response. The measure of FLC as amyloidogenic precursors is proven to be a robust marker of hematologic response, with a CR/VGPR being associated with improved outcomes.¹¹ A good hematologic response induces a significant reduction in the synthesis of harmful prefibrillar light chains and is associated with an increased likelihood of multiorgan ECV stabilization or even regression. With regards to markers of end-organ response, myocardial ECV regression was associated with a significant reduction in serum NT-proBNP, and liver ECV regression associated with a significant reduction in serum ALP. Furthermore, the changes in liver and spleen ECV in

FIGURE 4 Kaplan-Meier Curves Demonstrating the Prognostic Effect of Multiorgan Baseline ECVs and Treatment Response, Followed by a Univariable Cox Proportional Hazards Regression Analysis

(A) Kaplan-Meier curve comparing survival in patients with a normal myocardial ECV, mildly increased myocardial ECV, moderately increased myocardial ECV, and severely increased myocardial ECV at diagnosis. **(B)** Kaplan-Meier curve comparing survival in patients with a normal liver ECV subclinical increase in liver ECV and clinically significant increase in liver ECV at diagnosis. **(C)** Kaplan-Meier curve comparing survival in patients with a normal spleen ECV subclinical increase in spleen ECV and clinically significant increase in spleen ECV at diagnosis. Abbreviations as in [Figure 1](#).

TABLE 6 Univariable and Multivariable Analysis of Mortality Risk at Baseline and 6 Months After Commencing Chemotherapy

Survival Analysis at Baseline						
	Univariable		Multivariable Model Excluding Liver and Spleen ECV		Multivariable Model Including Liver and Spleen ECV	
	HR (95% CI)	P Value	HR (95% CI)	P Value	HR (95% CI)	P Value
NT-proBNP >1,800 ng/L	2.55 (1.76-3.72)	<0.001	1.43 (0.86-2.38)	0.170	1.65 (0.98-2.75)	0.058
Troponin T >40 ng/L	2.46 (1.69-3.58)	<0.001	1.49 (0.93-2.38)	0.100	1.35 (0.84-2.18)	0.210
dFLC >180 mg/L	1.76 (1.25-2.48)	0.001	1.58 (1.09-2.28)	0.014	1.45 (1.00-2.11)	0.050
Myocardial ECV	1.05 (1.03-1.07)	<0.001	1.04 (1.01-1.06)	0.001	1.03 (1.01-1.06)	0.009
Liver ECV	1.03 (1.01-1.05)	<0.001	–	–	1.03 (1.01-1.05)	0.001
Spleen ECV	1.01 (1.00-1.02)	0.244	–	–	0.99 (0.98-1.01)	0.347
Survival Analysis at 6 mo						
	Univariable		Multivariable Model Excluding Change in Liver and Spleen ECV		Multivariable Model Including Change in Liver and Spleen ECV	
	HR (95% CI)	P Value	HR (95% CI)	P Value	HR (95% CI)	P Value
Hematologic response						
CR	Ref.		Ref.		Ref.	
VGPR	1.80 (0.61-5.37)	0.289	1.48 (0.44-4.98)	0.526	1.18 (0.34-4.03)	0.794
PR	3.42 (1.36-8.57)	0.009	2.37 (0.83-6.76)	0.106	1.40 (0.43-4.48)	0.576
NR	8.70 (3.08-24.59)	<0.001	7.32 (2.55-21.05)	<0.001	3.84 (1.17-12.56)	0.026
NT-proBNP response						
Improvement	Ref.		Ref.		Ref.	
Stable	1.65 (0.57-4.76)	0.352	1.76 (0.50-6.15)	0.377	1.00 (0.28-3.64)	0.994
Worse	2.84 (1.08-7.48)	0.034	1.51 (0.49-4.68)	0.478	0.95 (0.29-3.12)	0.928
Change in myocardial ECV	1.13 (1.07-1.19)	<0.001	1.14 (1.06-1.23)	<0.001	1.11 (1.02-1.20)	0.011
Change in liver ECV	1.13 (1.09-1.17)	<0.001	–	–	1.07 (1.01-1.13)	0.014
Change in spleen ECV	1.07 (1.04-1.11)	<0.001	–	–	1.03 (0.98-1.08)	0.198

CR = complete response; dFLC = difference in concentration between aberrant and uninvolved class of free light chains; ECV = extracellular volume; NR = no response; NT-proBNP = N-terminal probrain natriuretic peptide; PR = partial response; Ref. = reference; VGPR = very good partial response.

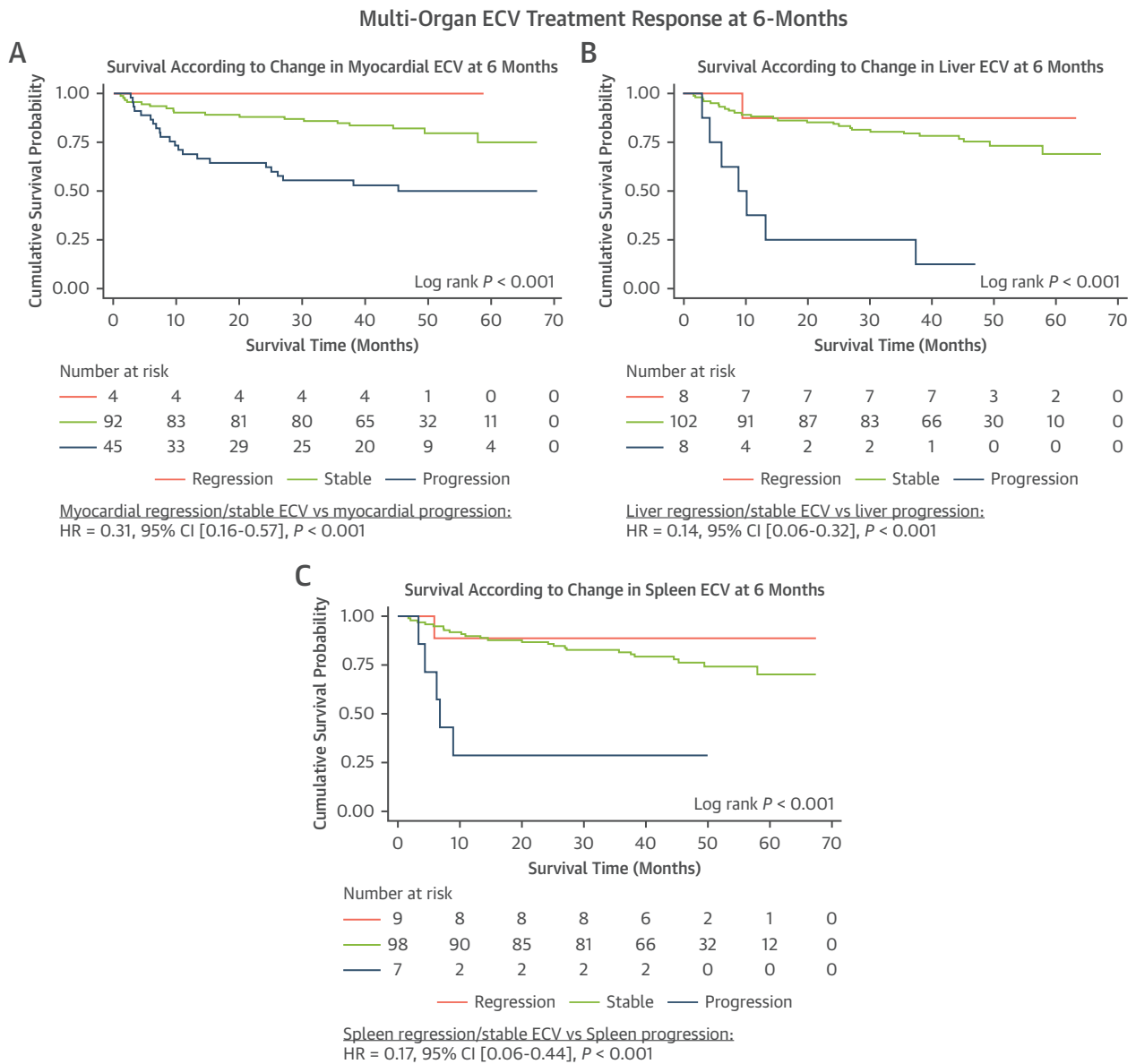
response to chemotherapy were corroborated against the changes in hepatic and splenic amyloid load, and demonstrated that changes in liver and spleen ECV accurately identified changes visceral organ amyloid load in the majority of cases. Considering the pathogenesis of amyloid deposition within the extracellular space, and the strong relationship between changes in ECV and traditional markers of treatment response, it is likely that multiorgan ECV changes reflect changes in the amyloid burden.

Multiorgan ECV mapping highlights the lag between hematologic response and organ regression. Although a deep hematologic response can be achieved rapidly, subsequent organ recovery may take months, evidenced by the increasing proportion of patients with multiorgan regression at each time point.

Multiorgan ECV regression began as early as 6 months, at which point a greater proportion of patients had liver and spleen regression than myocardial regression. However, at both 12 and 24 months, the proportion of patients with myocardial regression increased. This observation suggests organ recovery occurs at different rates, with the liver and spleen

regressing more rapidly than the heart. Hence, visceral organ ECV regression could be utilized as an early marker of treatment response, which commonly precedes myocardial ECV regression.

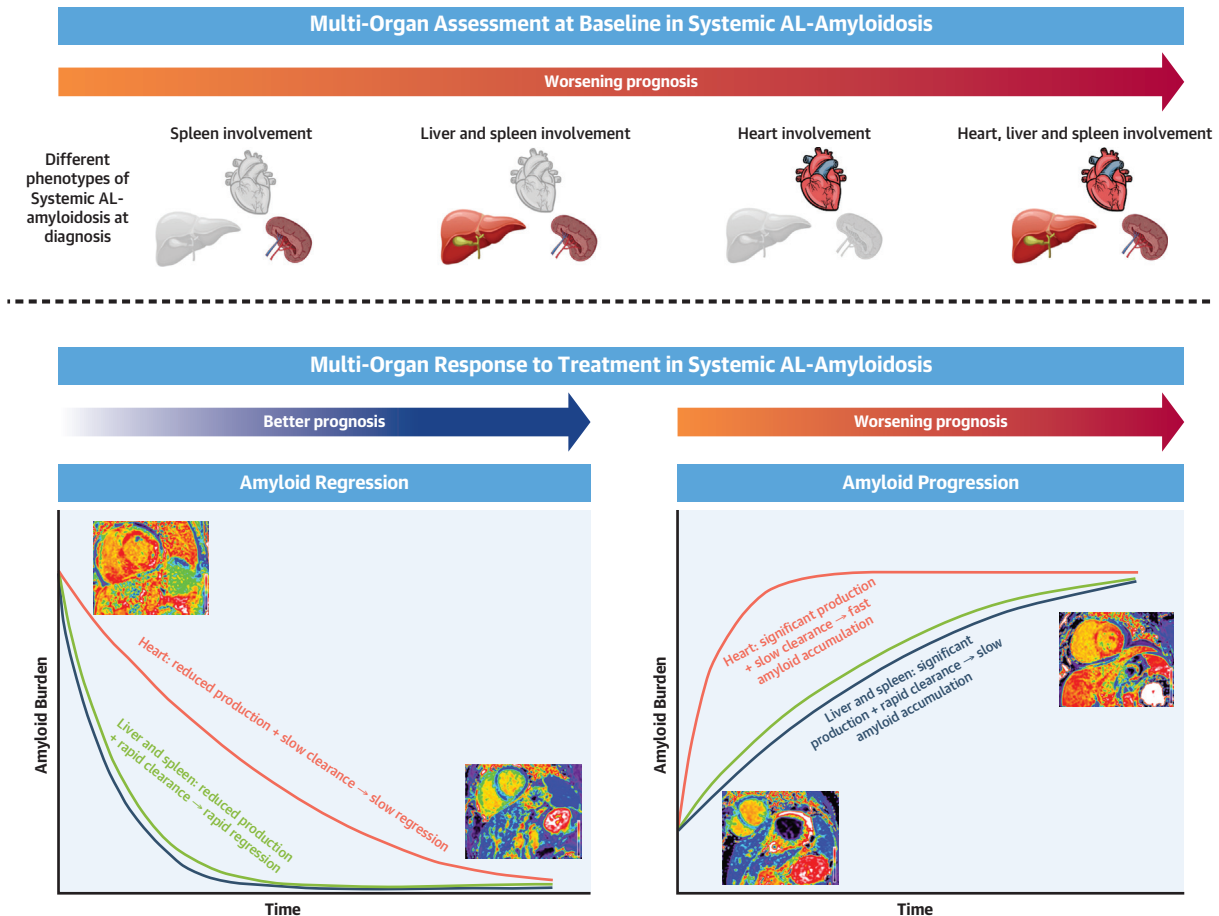
Amyloid accumulation is dynamic and involves constant turnover. Disease progression occurs when the rate of formation exceeds clearance, and regression vice versa.² At all 3 time points, only those with a good hematologic response demonstrated myocardial ECV regression, whereas 2 patients with a partial response demonstrated spleen ECV regression. Furthermore, a significant proportion of patients had myocardial ECV progression despite attaining a good hematologic response, whereas very few patients with a good hematologic response had liver or spleen ECV progression. In patients with a poor hematologic response, a far greater proportion displayed liver and spleen ECV stabilization than myocardial ECV stabilization. These findings support the notion that visceral organ recovery occurs more rapidly than cardiac recovery, and this may reflect a faster natural amyloid clearance in the visceral organs (**Central Illustration**).

FIGURE 5 Kaplan-Meier Curves Demonstrating the Prognostic Effect of the Change in Multiorgan ECVs in Response to Treatment at 6 Months, Followed by a Univariable Cox Proportional Hazards Regression Analysis

(A) Kaplan-Meier curve comparing survival in patients with myocardial regression, a stable myocardial ECV, and myocardial progression at 6 months. **(B)** Kaplan-Meier curve comparing survival in patients with liver regression, a stable liver ECV and liver progression at 6 months. **(C)** Kaplan-Meier curve comparing survival in patients with spleen regression, a stable spleen ECV and spleen progression at 6 months. Abbreviations as in [Figure 1](#).

ECV mapping complements conventional methods of monitoring treatment response by facilitating multiorgan assessment and the detection of disease progression despite a deep hematologic response; this scenario may result in additional treatment lines being utilized. Changes in myocardial, liver, and spleen ECV correlate with prognosis as early as

6 months after initiating chemotherapy. Multivariable analysis adjusting for hematologic response and change in NT-proBNP confirmed that changes in myocardial ECV and liver ECV remained independent predictors of mortality. This highlights the role of multiorgan ECV mapping in redefining treatment response beyond the reduction in FLC and NT-

CENTRAL ILLUSTRATION Patterns of Organ Infiltration at Diagnosis and Different Rates of Organ Regression and Progression in Response to TreatmentIoannou A, et al. *J Am Coll Cardiol Img.* 2023;■(■):■-■.

(Top) Worsening prognosis associated with different patterns of organ infiltration. **(Bottom)** Different rates of organ regression and progression in response to treatment, and the associated prognosis. AL = immunoglobulin light chain.

proBNP. Change in multiorgan ECV represents a novel and important addition to the standard measures of treatment response that could help clinicians tailor treatment to individual patients.

Furthermore, there are currently multiple novel monoclonal antibodies at various stages of development. These include birtamimab, CAEL-101, and AT-03, which are anticipated to promote regression by directly targeting amyloid fibrils and enhancing amyloid clearance.¹³⁻¹⁵ The ability to assess multiorgan response through a single imaging modality could be of great value as a clinical trial endpoint in the development of these medications.

STUDY LIMITATIONS. Technical limitations include a minority of ECVs not being measured because of

incomplete or absent imaging. Shimming was of the heart rather than visceral organs, which could lead to ECV measurement errors due to imperfect shim.⁸ This study utilized standard imaging from routine cardiac protocols. Future studies could explore whether dedicated imaging of the liver and spleen would provide better organ coverage. Serial ECV measurements were only available for patients with follow-up imaging. This invariably introduced a survival bias into the follow-up data. It may be the extent of differences is underestimated, eg, rapid amyloid accumulation may have resulted in the development of contraindications such as renal impairment or even resulted in death before the 6-month interval CMR scan could take place. The survival bias is likely to

have also impacted on the proportions of patients with multiorgan regression at each time point, with a lack of organ response inevitably increasing the risk of mortality. Finally, this is a single center study, and therefore our results require validation in a larger cohort of patients.

CONCLUSIONS

CMR-derived ECV mapping provides a comprehensive assessment of the multiorgan response to chemotherapy. Baseline myocardial and liver ECV and changes in myocardial and liver ECV independently predict mortality, even after adjusting for traditional prognosticators.

FUNDING SUPPORT AND AUTHOR DISCLOSURES

Dr Fontana is supported by a British Heart Foundation Intermediate Clinical Research Fellowship (FS/18/21/33447); and has consulting income from Intellia, Novo Nordisk, Pfizer, Eidos, Prothena, Akcea, Alnylam, Caleum, Alexion, Janssen, Ionis, and AstraZeneca. Dr Gilmore has received consulting income from Ionis, Eidos, Intellia, Alnylam, and Pfizer. Dr Wechelakar has received consulting income from Alexia, AstraZeneca, Janssen, Attralus, and Prothena. All other authors have reported that they have no relationships relevant to the contents of this paper to disclose.

ADDRESS FOR CORRESPONDENCE: Prof Marianna Fontana, National Amyloidosis Centre, University College London, Royal Free Hospital, Rowland Hill Street, London NW3 2PF, United Kingdom. E-mail: m.fontana@ucl.ac.uk.

PERSPECTIVES

COMPETENCY IN MEDICAL KNOWLEDGE: CMR-derived ECV measurements track changes in response to chemotherapy, with ECV changes most likely representing changes in the multiorgan amyloid burden. Myocardial and liver ECV at diagnosis and ECV changes 6 months after the initiation of treatment independently predict mortality.

TRANSLATIONAL OUTLOOK: The ability to assess multiorgan response through a single easily accessible imaging modality highlights the role of ECV mapping in redefining treatment response beyond the reduction in free light chains. ECV mapping could be of great value as a clinical trial endpoint, and in identifying patients with disease progression despite a good hematologic response.

REFERENCES

- Wechalekar AD, Gillmore JD, Hawkins PN. Systemic amyloidosis. *Lancet*. 2016;387:2641-2654.
- Hawkins PN, Lavender JP, Pepys MB. Evaluation of systemic amyloidosis by scintigraphy with 123I-labeled serum amyloid P component. *N Engl J Med*. 1990;323:508-513.
- Hawkins PN. Studies with radiolabelled serum amyloid P component provide evidence for turnover and regression of amyloid deposits in vivo. *Clin Sci (Lond)*. 1994;87:289-295.
- Rydh A, Suhr O, Hietala SO, Åhlström KR, Pepys MB, Hawkins PN. Serum amyloid P component scintigraphy in familial amyloid polyneuropathy: regression of visceral amyloid following liver transplantation. *Eur J Nucl Med*. 1998;25:709-713.
- Ioannou A, Patel RK, Razvi Y, et al. Multi-imaging characterization of cardiac phenotype in different types of amyloidosis. *J Am Coll Cardiol Img*. Published online August 13, 2022. <https://doi.org/10.1016/j.jcmg.2022.07.008>
- Ioannou A, Patel R, Gillmore JD, et al. Imaging-guided treatment for cardiac amyloidosis. *Curr Cardiol Rep*. 2022;24:839-850.
- Martinez-Naharro A, Patel R, Kotecha T, et al. Cardiovascular magnetic resonance in light-chain amyloidosis to guide treatment. *Eur Heart J*. 2022;43(45):4722-4735. <https://doi.org/10.1093/EURHEARTJ/EHAC363>
- Chacko L, Boldrini M, Martone R, et al. cardiac magnetic resonance-derived extracellular volume mapping for the quantification of hepatic and splenic amyloid. *Circ Cardiovasc Imaging*. 2021;314-324.
- Palladini G, Dispenzieri A, Gertz MA, et al. New criteria for response to treatment in immunoglobulin light chain amyloidosis based on free light chain measurement and cardiac biomarkers: impact on survival outcomes. *J Clin Oncol*. 2012;30:4541-4549.
- White SK, Sado DM, Fontana M, et al. T1 mapping for myocardial extracellular volume measurement by CMR: bolus only versus primed infusion technique. *J Am Coll Cardiol Img*. 2013;6:955-962.
- Kumar S, Dispenzieri A, Lacy MQ, et al. Revised prognostic staging system for light chain amyloidosis incorporating cardiac biomarkers and serum free light chain measurements. *J Clin Oncol*. 2012;30:989.
- Gertz MA, Comenzo R, Falk RH, et al. Definition of organ involvement and treatment response in immunoglobulin light chain amyloidosis (AL): a consensus opinion from the 10th International Symposium on Amyloid and Amyloidosis, Tours, France, 18-22 April 2004. *Am J Hematol*. 2005;79:319-328.
- O'Nuallain B, Allen A, Kennel SJ, Weiss DT, Solomon A, Wall JS. Localization of a conformational epitope common to non-native and fibrillar immunoglobulin light chains. *Biochemistry*. 2007;46:1240-1247.
- Wall JS, Kennel SJ, Williams A, et al. AL amyloid imaging and therapy with a monoclonal antibody to a cryptic epitope on amyloid fibrils. *PLoS One*. 2012;7(12):e52686. <https://doi.org/10.1371/journal.pone.0052686>
- Sirac C, Jaccard A, Codo R, et al. Pre-clinical characterization of a novel fusion protein (at-03), with pan-amyloid binding and removal. *Blood*. 2021;138:1207.

KEY WORDS cardiac magnetic resonance, extracellular volume mapping, systemic AL amyloidosis

APPENDIX For an expanded Results section and supplemental figures, please see the online version of this paper.